

# Bilayer Molecular Assembly at a Solid/Liquid Interface as Triggered by a Mild Electric Field\*\*

Qing-Na Zheng, Xuan-He Liu, Xing-Rui Liu, Ting Chen, Hui-Juan Yan, Yu-Wu Zhong, Dong Wang,\* and Li-Jun Wan\*

**Abstract:** The construction of a spatially defined assembly of molecular building blocks, especially in the vertical direction, presents a great challenge for surface molecular engineering. Herein, we demonstrate that an electric field applied between an STM tip and a substrate triggered the formation of a bilayer structure at the solid–liquid interface. In contrast to the typical high electric-field strength ( $10^9 \text{ V m}^{-1}$ ) used to induce structural transitions in supramolecular assemblies, a mild electric field ( $10^5 \text{ V m}^{-1}$ ) triggered the formation of a bilayer structure of a polar molecule on top of a nanoporous network of trimesic acid on graphite. The bilayer structure was transformed into a monolayer kagome structure by changing the polarity of the electric field. This tailored formation and large-scale phase transformation of a molecular assembly in the perpendicular dimension by a mild electric field opens perspectives for the manipulation of surface molecular nanoarchitectures.

The controllable structural transformation of molecular nanoarchitectures in response to external stimuli has received considerable attention, as it promises practical yet effective means to modulate the functionality of surfaces and interfaces.<sup>[1]</sup> Scanning tunneling microscopy (STM) can act not only as a tool for visualizing the structural evolution but also as an external stimulant. From a mechanistic point of view, the stimulation executed by the STM tip can be categorized into an electronic effect and an electric-field effect. The electron current tunneling between the STM tip and the surface can

excite reactions or movements of a single molecule.<sup>[1b,2]</sup> Kudernac et al. demonstrated that a four-wheeled molecule can be propelled on a Cu(111) surface by the excitation of inelastic electrons.<sup>[1b]</sup> Dujardin and co-workers reported that selective electron-induced reactions of individual biphenyl molecules can be induced by injecting or removing tunneling electrons: removal from the adsorbates or injection into adsorbates.<sup>[2b]</sup> On the other hand, although rarely reported, the electric field between the STM tip and the substrate can act as a “trigger” to induce the structural transition of surface supramolecular assemblies.<sup>[3]</sup> For example, Alemani et al. reported that the *trans*–*cis* configuration transformation of azobenzene can be controlled by changing the local electric field under the STM tip, without the tunneling of electrons.<sup>[3a]</sup> Recently, Mali et al. showed that it was possible to drive the large-scale reversible transformation of the two distinct assembly phases of a positively charged polycyclic aromatic hydrocarbon by applying voltage pulses to the STM tip.<sup>[3c]</sup> Generally, the existence of a threshold bias is characteristic for tunneling-electron-induced structural transformation, whereas processes triggered by an electric field (typically in the order of  $10^9 \text{ V m}^{-1}$ ) do not depend on the threshold voltage. Moreover, as the number of tunneling electrons decreases exponentially with the distance between the STM tip and adsorbates, the electronic excitation generally requires direct contact with or the vibrational excitation of a single adsorbate. In contrast, electric-field-induced processes can occur at quite a large distance away from the STM tip. Nevertheless, in most cases of electric-field-induced processes, the electric field has been induced by changing the bias of imaging or applying a pulse to the STM tip during scanning by the STM tip. Therefore, a high electric-field strength has been applied (in the order of magnitude of  $10^9 \text{ V m}^{-1}$ ) because of the nanometer-scale distance between the STM tip and adsorbates.<sup>[2a–c,3a,b,e]</sup>

Surface molecular engineering aims at spatially controlling the assembly of molecular building blocks in a designed arrangement.<sup>[4]</sup> Despite extensive studies on the lateral organization of functional molecules, control in the vertical direction (i.e., that perpendicular to the basal plane of the substrate) is still relatively poor.<sup>[5]</sup> Knowledge about the extension of the self-assembly process to the third dimension is important for crystal growth and organic molecular devices.<sup>[6]</sup> The multilayer supramolecular architecture can be tailored by appropriate supramolecular interactions, such as  $\pi$ – $\pi$  stacking and electrostatic interactions. For example, Ciesielski et al. obtained bilayer kagome networks by taking advantage of hydrogen-bond recognition and  $\pi$ – $\pi$  stacking of the planar building blocks.<sup>[5d]</sup> Instead of using passive loading

[\*] Q.-N. Zheng, X.-H. Liu, X.-R. Liu, T. Chen, H.-J. Yan, Prof. Dr. D. Wang, Prof. Dr. L.-J. Wan  
Key Laboratory of Molecular Nanostructure and Nanotechnology  
Institute of Chemistry, Chinese Academy of Sciences  
and Beijing National Laboratory for Molecular Sciences  
Beijing 100190 (P.R. China)  
E-mail: wangd@iccas.ac.cn  
wanlijun@iccas.ac.cn

Q.-N. Zheng, X.-H. Liu, X.-R. Liu  
University of the Chinese Academy of Sciences (China)  
Y.-W. Zhong  
Beijing National Laboratory for Molecular Sciences  
CAS Key Laboratory of Photochemistry, Institute of Chemistry  
Chinese Academy of Sciences  
Beijing 100190 (P.R. China)

[\*\*] This research is supported by the National Key Project on Basic Research (grants 2011CB808700 and 2011CB932300), the National Natural Science Foundation of China (grants 91023013, 21127901, 21121063, 91227104, and 21233010), and the Strategic Priority Research Program of the Chinese Academy of Sciences (Grant No. XDB12020100).

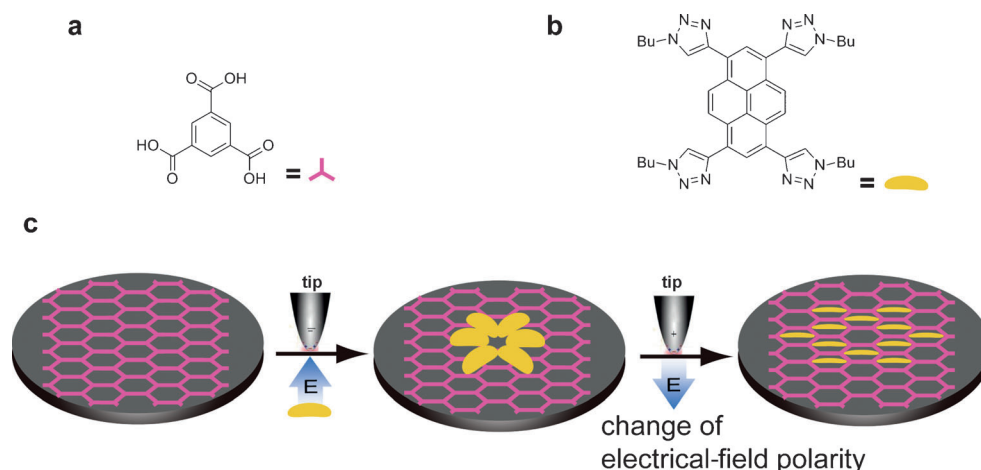
Supporting information for this article is available on the WWW under <http://dx.doi.org/10.1002/anie.201406523>.

molecules on the underlayer, Beton and co-workers demonstrated that the nonplanar guest C<sub>60</sub> induced tetracarboxylic acid (TCA) derivatives to form a bilayer architecture.<sup>[7]</sup> Generally speaking, there is a shortage of supramolecular synthons available for controllable vertical assembly, as compared to those known to control 2D in-plane assembly. Therefore, it is desirable to develop an effective way to precisely control supramolecular assembly in the vertical direction.

Herein, we demonstrate the growth of a hetero-bilayer supramolecular structure by modulation by a mild electric field. We found that an electric-field strength of about 10<sup>5</sup> V m<sup>-1</sup> (four orders of magnitude lower than the typical field strength used in other reported studies) is enough to induce the formation of a hetero-bilayer structure of 1,3,6,8-tetrakis(1-butyl-1*H*-1,2,3-triazol-4-yl)pyrene (TP) molecules on top of a trimesic acid (TMA) matrix.<sup>[8]</sup> The chemical structures of TP and TMA are shown in Scheme 1 a,b. The bilayer structure is a metastable phase that can be transformed into a kagome structure<sup>[9]</sup> by changing the polarity of the electric field (Scheme 1 c). The modulation of the growth and transformation of a bilayer structure by a mild electric field offers a new possibility for manipulation in surface supramolecular chemistry.

The self-assembly of TMA molecules from a solution in octanoic acid (OA) at a highly oriented pyrolytic graphite (HOPG) surface led to a honeycomb structure (Figure 1 a). The TMA honeycomb structure had a periodicity of 1.6 nm, in good agreement with previous reports.<sup>[10]</sup> The typical domain size can reach 200 × 200 nm<sup>2</sup>.

A bilayer “flower structure” of TP molecules on the top of the TMA honeycomb network was fabricated under the control of a positive electric field (from the substrate to the tip; see experimental details in the Supporting Information). The resulting large-scale supramolecular structure consisted of an array of flower-shaped clusters with hexagonal symmetry (Figure 1 b). Each flower-shaped cluster was composed of six hexagonally arranged “petals”. By STM, each petal appeared as an ellipse with a diameter of 1.2 nm and a corrugation height of 0.16 nm, in agreement with the size of the TP molecule. The domain size of the flower structure typically reached 200 × 200 nm<sup>2</sup>. The upper layer consisting of the TP flower structure was oriented at an angle of 30° with respect to the TMA layer below (see Figure S3 in the Supporting Information), thus suggesting that the symmetry of the TMA network affects the organization of the upper-layer TP flower



**Scheme 1.** Electric-field-induced formation of a bilayer flower structure of TP on a TMA network. a) Chemical structure of TMA. The TMA molecule is schematically represented by a pink trefoil. b) Chemical structure of TP. The TP molecule is represented by a yellow spot. c) Illustration of the electric-field-induced formation of a bilayer flower and the phase transition from the bilayer flower structure to the monolayer kagome structure.

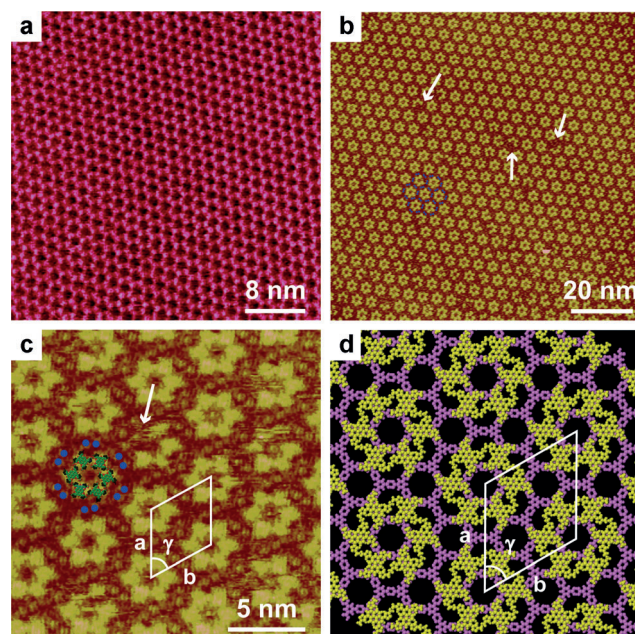


**Figure 1.** Formation of the flower structure by stimulation with an electric field. a) Large-scale STM image of the honeycomb TMA adlayer. Tunneling conditions:  $V_{\text{bias}} = 700$  mV,  $I_t = 450$  pA. b) Large-scale STM image of the electric-field-induced bilayer flower structure. Tunneling conditions:  $V_{\text{bias}} = 561$  mV,  $I_t = 605$  pA. c) High-resolution STM image of the bilayer structure. Tunneling conditions:  $V_{\text{bias}} = 758$  mV,  $I_t = 357$  pA. d) Tentatively proposed structural model of the flower structure. TP and TMA molecules are colored yellow and purple, respectively.

structure. Some defects with missed petals can be clearly seen in the STM image, as indicated by arrows in Figure 1 b,c.

There are some less bright spots dispersed in the positions of the missing petals, as indicated by the arrow in Figure 1 c. These spots are ascribed to TMA molecules. The existence of TMA in positions underneath TP molecules suggests that the



TMA matrix serves as an underlayer for accommodating TP molecules. Furthermore, less bright features dispersed in the interstice between hexagonal flowers are visible, as indicated by blue spots. The less bright spots are also ascribed to TMA molecules. The periodicity of the flower structure ( $(4.9 \pm 0.2)$  nm) corresponds to 3 times the periodicity of the TMA honeycomb template ( $(1.6 \pm 0.1)$  nm), thus suggesting an unperturbed structure of the TMA honeycomb network after the accommodation of TP molecules. Six TP petals make up a flower-shaped cluster, as illustrated by the overlaid model in Figure 1c. Meanwhile, two TMA molecules are positioned at each of the six sides of a flower, as illustrated by blue spots surrounding the overlaid model. Two neighboring flowers share two such TMA molecules as a border. Some fuzzy lines across the clusters appear on the STM image, thus suggesting that the adsorbates are unstable under STM scanning. Figure 1d shows the proposed structural model. No obvious directional intermolecular interaction exists in the upper layer. TP molecules may interact through a non-specific van der Waals force to form a commensurate array of flower clusters on top of the TMA network.

In contrast, a kagome structure forms when no electric field or a negative electric field is applied during the assembly process. A well-ordered kagome network can be clearly seen in Figure 2. Each TP molecule appears as an ellipse with a well-defined orientation. The TP molecules are trapped alternately in the pores of the TMA network. The parameters of the unit cell outlined in Figure 2b are  $a = b = (4.0 \pm 0.2)$  nm and  $\gamma = (60 \pm 2)^\circ$ .<sup>[9]</sup>

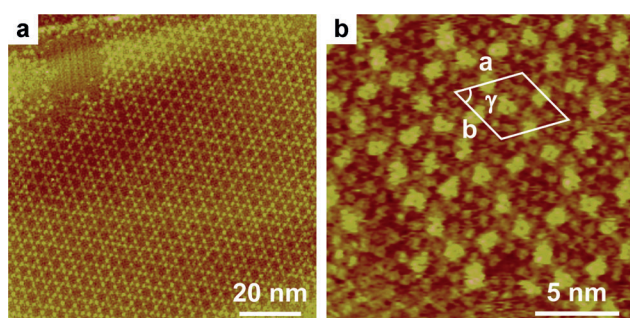


**Figure 2.** Formation of the kagome structure without an electric-field stimulus. a) Kagome structure formed by the coassembly of TP and TMA. Tunneling conditions:  $V_{\text{bias}} = 693$  mV,  $I_t = 500$  pA. b) High-resolution STM image of the kagome structure. Tunneling conditions:  $V_{\text{bias}} = 770$  mV,  $I_t = 320$  pA.

Topographic cross-sections of the flower structure and the kagome structure are shown in Figure 3. The apparent heights of an individual TP molecule and an individual TMA molecule were measured to be 1.6 and 0.5 Å, respectively, and a margin height difference of about 1.0 Å was found (Figure 3a). In contrast, a lower apparent height margin (0.5 Å) was found between individual TP (1.0 Å) and TMA molecules (0.5 Å) in the kagome monolayer (Figure 3b). Cross-section analysis indicated that the TP molecules were stacked on the underlying TMA adlayer to form a bilayer structure in the flower structure, whereas the kagome structure is a monolayer structure.

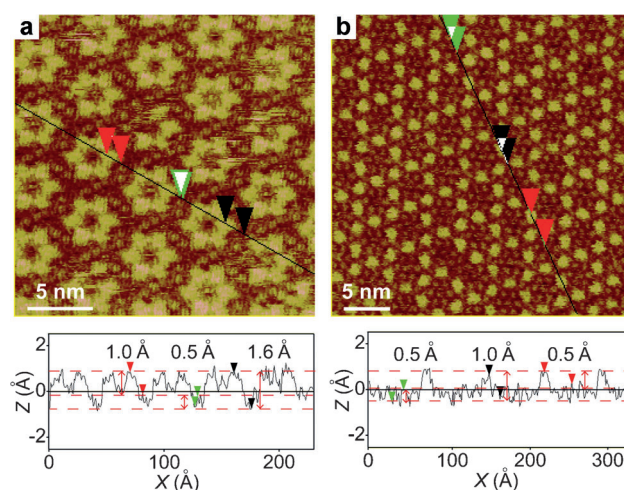


**Figure 3.** Height profiles for the bilayer flower structure and the kagome structure. a) Bilayer flower structure. b) Kagome structure. The height profile  $Z$  is taken along the line  $X$  in the STM image of the corresponding structure. The location of the height profile is marked with a black line on the magnified STM image.

Although the formation of a bilayer structure was induced by an electric field, we found that the structure underwent a phase transition to a kagome structure immediately when the direction of the electric field was changed. Figure 4a shows the initial flower bilayer structure. The polarity of the applied electric field was then changed rapidly (Figure 4a,b). Fuzzy features that can be seen in the STM image in Figure 4b may be due to the immediate change in the molecular assembly upon the change in the electric-field polarity. Once the STM system was drift-stable, the bilayer flower structure no longer existed on the surface. The transformation process from a bilayer flower structure to a monolayer kagome structure was recorded in subsequent images of the same region (Figure 4b–f). After several minutes, a few triangular building blocks, as indicated by arrows in Figure 4d, began to expand to generate a domain with a kagome structure. A domain with a kagome structure can be clearly seen in Figure 4e and in the magnified STM image in Figure 4f.

We carried out a series of control experiments to investigate the effect of an electric field on the adsorption behavior of the bilayer flower structure. First, it was found that the assembly behavior of pure TP or TMA molecules was not affected by an electric field (see Figures S1 and S2). We then found that the formation of the flower structure depended on the electric field (both the bias and the distance between the STM tip and the substrate; see Figures S5 and S6). More specifically, the application of a positive electric field (from the substrate to the tip) of an appropriate field strength during the preparation process is critical to induce the formation of the bilayer structure (see Figure S7). On the other hand, the kagome structure can form with no electric field or with a negative electric field. Once the adsorbates are stable, the bilayer flower structure is sensitive to the electric-field polarity. The flower structure is energetically unfavorable and can be converted into the kagome structure (see Figures S8 and S10). In contrast, the kagome structure is

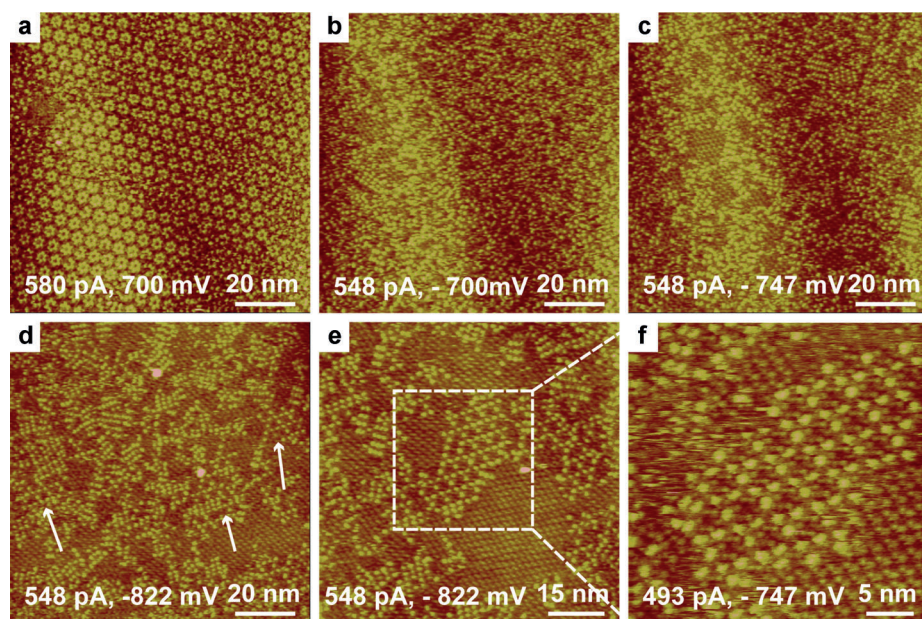


**Figure 4.** Consecutive STM images of the bilayer flower in response to changes in the polarity of the electric field. a) Initial bilayer flower structure. b–e) STM images of the phase transition from the bilayer flower structure to the monolayer kagome structure. f) Magnified STM image of the selected area in (e). All images were observed in 3 min and show the same region. Tunneling conditions are indicated on each image.

a stable assembly structure that is not affected by an electric field (see Figure S9). Overall, the system provides an example of a transformation from a nonplanar to a planar supramolecular structure through the reversal of an electric field.

To further clarify the formation mechanism of the bilayer structure under electric-field modulation, we carried out a series of control experiments. Since a saturated solution of TMA molecules in OA was applied to the substrate, there were a large number of excess TMA molecules at the solid–liquid interface. We found that a similar bilayer flower structure could be formed by replacing the excess TMA with another protic acid, such as  $\text{CF}_3\text{COOH}$ , under similar conditions of electric-field control (see Figures S11 and S12). However, the bilayer flower structure could not be formed in a neutral or basic environment (see Figures S13 and S14). The experiments demonstrated that an acidic environment and an electric field are required for the formation of a bilayer flower structure. According to previous reports,<sup>[11–13]</sup> a triazole moiety is prone to undergo protonation in an acidic environment. We propose that the TP molecules are protonated in an acidic environment and that the charged TP molecules align to form a vertical hetero-bilayer structure on top of the TMA network under the positive electric field. When the polarity of the electric field is changed, the orientation effect of the electric field is reversed, and the bilayer structure cannot be sustained. Instead, a phase transition to a monolayer kagome structure is observed. Overall, variation of the direction of the electric-field surrounding the adsorbates can act as a “trigger” to induce molecular motion and then prompt large-scale assembly transformation.

In conclusion, we have demonstrated the growth of a specific bilayer structure under a mild electric field. The electric-field strength had a magnitude of the order  $10^5 \text{ V m}^{-1}$ , which is much smaller than that used in previously reported studies (about  $10^9 \text{ V m}^{-1}$ ). The bilayer flower structure responded in a sensitive manner to the external electric field of the STM tip. A structure transformation from the bilayer flower structure to a monolayer kagome structure was triggered by changing the polarity of the electric field. We envision that this structural transition promoted by a low electric field could be realized at a macroscopic level. The structural switchability and controllability of the supramolecular assembly system under the influence of a mild electric field also provides insight into the manipulation of self-assembly processes and opens up a door to the for-

mation of 3D crystals from a 2D surface.

Received: June 24, 2014

Revised: October 9, 2014

Published online: November 6, 2014

**Keywords:** bilayers · electric fields · kagome structure · scanning tunneling microscopy · self-assembly

- [1] a) F. Chiaravallotti, L. Gross, K.-H. Rieder, S. M. Stojkovic, A. Gourdon, C. Joachim, F. Moresco, *Nat. Mater.* **2007**, *6*, 30–33; b) T. Kudernac, N. Ruangsapapichat, M. Parschau, B. Maciá, N. Katsonis, S. R. Harutyunyan, K.-H. Ernst, B. L. Feringa, *Nature* **2011**, *479*, 208–211; c) G. Vives, J. M. Tour, *Acc. Chem. Res.* **2009**, *42*, 473–487.
- [2] a) S. Clair, O. Ourdjini, M. Abel, L. Porte, *Chem. Commun.* **2011**, *47*, 8028–8030; b) D. Riedel, M.-L. Bocquet, H. Lesnard, M. Lastapis, N. Lorente, P. Sonnet, G. Dujardin, *J. Am. Chem. Soc.* **2009**, *131*, 7344–7352; c) P. A. Sloan, R. Palmer, *Nature* **2005**, *434*, 367–371; d) A. Nickel, R. Ohmann, J. Meyer, M. Grisolia, C. Joachim, F. Moresco, G. Cuniberti, *ACS Nano* **2013**, *7*, 191–197; e) Y. Jiang, Q. Huan, L. Fabris, G. C. Bazan, W. Ho, *Nat. Chem.* **2013**, *5*, 36–41; f) D. den Boer, M. Li, T. Habets, P. Iavicoli, A. E. Rowan, R. J. Nolte, S. Speller, D. B. Amabilino, S. De Feyter, J. A. Elemans, *Nat. Chem.* **2013**, *5*, 621–627.
- [3] a) M. Alemani, M. V. Peters, S. Hecht, K.-H. Rieder, F. Moresco, L. Grill, *J. Am. Chem. Soc.* **2006**, *128*, 14446–14447; b) S. L. Lee, Y. J. Hsu, H. J. Wu, H. A. Lin, H. F. Hsu, C. H. Chen, *Chem. Commun.* **2012**, *48*, 11748–11750; c) I.-W. Lyo, P. Avouris, *Science* **1991**, *253*, 173–176; d) A. Cristadoro, M. Ai, H. J. Räder, J. P. Rabe, K. Müllen, *J. Phys. Chem. C* **2008**, *112*, 5563–5566; e) K. S. Mali, D. Wu, X. Feng, K. Müllen, M. Van der Auweraer, S. De Feyter, *J. Am. Chem. Soc.* **2011**, *133*, 5686–5688.



- [4] a) K. S. Mali, J. Adisojoso, E. Ghijsens, I. De Cat, S. De Feyter, *Acc. Chem. Res.* **2012**, *45*, 1309–1320; b) A. Ciesielski, C.-A. Palma, M. Bonini, P. Samorì, *Adv. Mater.* **2010**, *22*, 3506–3520; c) A. G. Slater, P. H. Beton, N. R. Champness, *Chem. Sci.* **2011**, *2*, 1440–1448; d) T. Kudernac, S. Lei, J. A. Elemans, S. De Feyter, *Chem. Soc. Rev.* **2009**, *38*, 402–421; e) X. M. Zhang, Q. D. Zeng, C. Wang, *Chem. Asian J.* **2013**, *8*, 2330–2340; f) J. V. Barth, G. Costantini, K. Kern, *Nature* **2005**, *437*, 671–679; g) J. A. Theobald, N. S. Oxtoby, M. A. Phillips, N. R. Champness, P. H. Beton, *Nature* **2003**, *424*, 1029–1031; h) J. W. Colson, W. R. Dichtel, *Nat. Chem.* **2013**, *5*, 453–465.
- [5] a) O. Ivasenko, J. M. MacLeod, K. Y. Chernichenko, E. S. Balenkova, R. V. Shpanchenko, V. G. Nenajdenko, F. Rosei, D. F. Perepichka, *Chem. Commun.* **2009**, 1192–1194; b) N. Crivillers, S. Furukawa, A. Minoia, A. Ver Heyen, M. Mas-Torrent, C. Sporer, M. Linares, A. Volodin, C. Van Haesendonck, M. Van der Auweraer, *J. Am. Chem. Soc.* **2009**, *131*, 6246–6252; c) K. M. Koczur, E. M. Hamed, A. Houmam, *Langmuir* **2011**, *27*, 12270–12274; d) A. Ciesielski, A. Cadetdu, C.-A. Palma, A. Gorczyński, V. Patroniak, M. Cecchini, P. Samorì, *Nanoscale* **2011**, *3*, 4125–4129.
- [6] a) S. Roquet, A. Cravino, P. Leriche, O. Alévêque, P. Frère, J. Roncali, *J. Am. Chem. Soc.* **2006**, *128*, 3459–3466; b) L. F. Dössel, V. Kamm, I. A. Howard, F. Laquai, W. Pisula, X. Feng, C. Li, M. Takase, T. Kudernac, S. De Feyter, K. Müllen, *J. Am. Chem. Soc.* **2012**, *134*, 5876–5886.
- [7] a) M. O. Blunt, J. C. Russell, M. d. C. Gimenez-Lopez, N. Taleb, X. Lin, M. Schroder, N. R. Champness, P. H. Beton, *Nat. Chem.* **2011**, *3*, 74–78; b) S. De Feyter, *Nat. Chem.* **2011**, *3*, 14–15.
- [8] L. Wang, W.-W. Yang, R.-H. Zheng, Q. Shi, Y.-W. Zhong, J.-N. Yao, *Inorg. Chem.* **2011**, *50*, 7074–7079.
- [9] Q.-N. Zheng, L. Wang, Y.-W. Zhong, X.-H. Liu, T. Chen, H.-J. Yan, D. Wang, J. Yao, L.-J. Wan, *Langmuir* **2014**, *30*, 3034–3040.
- [10] a) S. Griessl, M. Lackinger, M. Edelwirth, M. Hietschold, W. M. Heckl, *Single Mol.* **2002**, *3*, 25–31; b) S. J. Griessl, M. Lackinger, F. Jamitzky, T. Markert, M. Hietschold, W. M. Heckl, *J. Phys. Chem. B* **2004**, *108*, 11556–11560; c) M. Lackinger, S. Griessl, W. M. Heckl, M. Hietschold, G. W. Flynn, *Langmuir* **2005**, *21*, 4984–4988.
- [11] a) I. Blakey, L. Chen, B. Dargaville, H. Liu, A. Whittaker, W. Conley, E. Piscani, G. Rich, A. Williams, P. Zimmerman, *Proc. SPIE* **2007**, *6519*, 651909; b) S. Živanović, Bachelor Thesis, TBU in Zlín, Faculty of Technology, **2013**, pp. 1–45.
- [12] a) F. Herbstein, M. Kapon, *Acta Crystallogr., Sect. B* **1979**, *35*, 1614–1619; b) F. Herbstein, M. Kapon, I. Maor, G. Reisner, *Acta Crystallogr., Sect. B* **1981**, *37*, 136–140; c) F. Herbstein, R. Marsh, *Acta Crystallogr., Sect. B* **1977**, *33*, 2358–2367.
- [13] a) J. L. M. Abboud, C. Foces-Foces, R. Notario, R. E. Trifonov, A. P. Volovodenco, V. A. Ostrovskii, I. Alkorta, J. Elguero, *Eur. J. Org. Chem.* **2001**, 3013–3024; b) I. Bratko, G. Guisado-Barrios, I. Favier, S. Mallet-Ladeira, E. Teuma, E. Peris, M. Gómez, *Eur. J. Org. Chem.* **2014**, 2160–2167; c) R. Subbaraman, H. Ghassemi, T. Zawodzinski, Jr., *Solid State Ionics* **2009**, *180*, 1143–1150.